Arabian Journal for Science and Engineering
https://doi.org/10.1007/s13369-018-3086-5

RESEARCH ARTICLE - CIVIL ENGINEERING

Theoretical Analysis of Thermal Behavior of Overlapped GFRP Bars Embedded in Reinforced Concrete Beams

H. Bellakehal[1] · A. Zaidi[1] · K. Mouattah[1] · R. Masmoudi[2] · M. Bencheriet[1,3] · A. Boutaiba[1,3]

Received: 10 March 2017 / Accepted: 30 December 2017

Abstract

Fiber-reinforced polymer (FRP) bars are being increasingly used in civil engineering constructions due to their excellent properties in comparison with steel bars, especially in terms of corrosion resistance. Designers generally adopt over-reinforced sections to avoid a sudden failure mode of FRP bars. Therefore, the overlap of the bars is omnipresent. However, under large temperature increase, the overlap area may be regarded as a zone of radial stress concentration generated by a pressure caused by the thermal expansion of both bars. Several studies have been conducted on the thermal behavior of FRP bars-reinforced concrete elements, but none of these studies has taken into account the overlapping effect of bars under high temperature. The aim of this study is to develop numerical and analytical models to predict transverse thermal strains and stresses in FRP bars interaction zone by varying the ratio of concrete cover thickness to FRP bar diameter (c/d_{b}) from 1 to 3.2, and the temperature increases from 0 to $+60\,^{\circ}\mathrm{C}$ for concrete beams reinforced with two overlapped glass FRP (GFRP) bars. The numerical model is developed using ADINA finite element software, and its results are compared with those obtained from the analytical model based on linear elasticity theory.

Keywords Bars interaction · Temperature · Overlapped GFRP bars · Concrete cover · Radial pressure · Transverse stresses · Transverse strains

1 Introduction

During the 1970s, the composites of fiber-reinforced polymers (FRP) were introduced in the sector of civil engineering construction. They have become one of the most effective solutions to steel corrosion problem because of their high resistance to corrosion and their peculiar mechanical and physical properties [1]. Compared to concrete sections reinforced with steel bars, concrete sections reinforced with FRP bars are characterized by lack ductility and high deformability; therefore, all concrete sections reinforced with FRP bars must be designed so that the rupture of the section occurs by the crushing of concrete in compression [2]. This means that the concrete sections must be over-reinforced. To meet this requirement, the overlap of bars is generally omnipresent in FRP bars-reinforced concrete sections. Under large temperature increase, the region of overlapped bars may be regarded as a zone of tensile stress concentration generated by the radial pressure caused by the transverse thermal expansion of the overlapped bars. It should be noted that the main drawback of FRP reinforcing system is the lack of thermal compatibility between concrete and bars, particularly in the transverse direction. These tensile stresses may cause splitting cracks within concrete and, subsequently, the degradation of the member stiffness. As a result of the appearance of the first cracks within concrete, important

✉ H. Bellakehal
Hizia.Bellakehal@USherbrooke.ca

A. Zaidi
Ali.Zaidi@USherbrooke.ca

K. Mouattah
k.mouattah@mail.lagh-univ.dz

R. Masmoudi
RadhouaneMasmoudi@USherbrooke.ca

M. Bencheriet
sadbench@gmail.com

A. Boutaiba
boudz17@gmail.com

1 Structures Rehabilitation and Materials Laboratory (SREML), University of Laghouat, BP 37, 03000 Laghouat, Algeria

2 Department of Civil Engineering, University of Sherbrooke, Sherbrooke, QC, Canada

3 University of Laghouat, Laghouat, Algeria

Published online: 24 January 2018

Table 1 Geometrical and mechanical properties of GFRP bars-reinforced concrete beams

Beam designation	Width b' (mm)	Height h (mm)	Bar diameter d_b (mm)	Concrete cover c (mm)	c/d_b	f_{fu}(MPa)	E_l (GPa)	ε_{lu} (%)
P.#10.20[a]	76	100	9.5	20	2.1	627	42	1.8
P.#10.25	76	100	9.5	25	2.6	627	42	1.8
P.#10.30	76	100	9.5	30	3.2	627	42	1.8
P.#13.20	76	100	12.7	20	1.6	617	42	1.5
P.#13.25	76	100	12.7	25	2.0	617	42	1.5
P.#13.30	76	100	12.7	30	2.4	617	42	1.5
P.#16.20	76	100	15.9	20	1.3	535	42	1.4
P.#16.25	76	100	15.9	25	1.6	535	42	1.4
P.#16.30	76	100	15.9	30	1.9	535	42	1.4
P.#19.20	100	125	19.1	20	1.0	600	40	1.5
P.#19.25	100	125	19.1	25	1.3	600	40	1.5
P.#19.30	100	125	19.1	30	1.6	600	40	1.5
P.#25.25	100	150	25.4	25	1.0	N/A[b]	N/A	N/A
P.#25.30	100	150	25.4	30	1.2	N/A	N/A	N/A
P.#25.35	100	150	25.4	35	1.4	N/A	N/A	N/A

[a]P.#10.20: refers to beam reinforced with GFRP bar number 10 and having a concrete cover thickness of 20 mm.
[b]N/A: mean not available

thermal strains take place when the thermal stress in the concrete around the glass FRP (GFRP) bars in different locations reaches its tensile strength (f_t). The resulting thermal cracks cause the loss of the bond between GFRP bar and the surrounding concrete and, eventually, the failure of the concrete cover if the concrete confining action is not sufficient [1,3–5]. Several studies have been carried out on the thermal behavior of FRP bars-reinforced concrete elements, but none of them has taken into consideration the overlapping effect of bars under high temperature [5–8]. This study is meant to analyze theoretically the behavior of concrete beams reinforced with two overlapped GFRP bars by developing numerical and analytical models. The numerical model is based on the finite element method, using ADINA nonlinear analysis software which has been used in several researches and has given a good correlation with the experimental tests [8–11]. The developed analytical model is based on linear elasticity theory using Timoshenko equations [9] for a hollow cylinder under internal hydrostatic pressure. The results of this study allow determining the effect of vertical overlapping of FRP bars anchored in the concrete on the transverse tensile stresses and strains of prismatic reinforced concrete beams under temperatures varying from 0 to + 60 °C, which represents, generally, higher global temperature variation in many countries. These strains are helpful in evaluating the temperature variation producing the first crack in concrete (ΔT_{cr}) at FRP bar/concrete interface and at the interaction zone of both bars. Moreover, such strains allow the evaluation of the temperature variation that produces the total failure of concrete cover (ΔT_{sp}) as a function of concrete cover thickness to FRP bar diameter ratio (c/d_b). The numerical results are in line with the analytical results for thermal loads less than cracking thermal loads.

2 Numerical Model

The numerical model is based on the finite element method using ADINA software. It is designed to study the effect of vertical overlap of two GFRP bars on the behavior of reinforced concrete beams under large temperature increase. This study, which is based on material nonlinearity analysis, investigates the transverse thermal stresses in the concrete cover and FRP bars by changing the temperature variation (ΔT) from 0 to + 60 °C and the concrete cover thickness to FRP bar diameter ratio (c/d_b). It also allows to determine the temperature variation (ΔT_{cr}) producing the first crack in the concrete at the FRP bar/concrete interface in the interaction zone of both bars and the temperature variation producing the failure of concrete cover (ΔT_{sp}) as a function of the ratio (c/d_b). All beams have a constant length of 380 mm and a variable transverse section (hxb’). Further details of beams are shown in Table 1 and Fig. 1. The selected concrete covers were chosen to obtain a wide range of concrete cover thickness to FRP bar diameter (c/d_b) ratio ranging from 1.0 to 3.2.

Considering the fact that the axial strains of the beams are constant, beams were modeled by means of two-dimensional plane stress elements, using triangular finite elements of six nodes (Fig. 1). As shown in Fig. 1, the study was carried

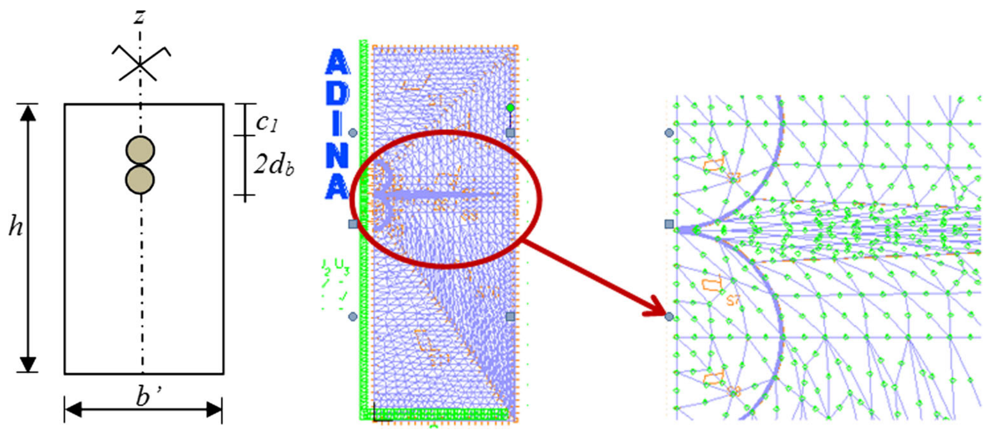

Fig. 1 Geometry and meshing diagram of a cross section of concrete beam reinforced with two GFRP bars

out for the half cross section of beams since the beams are symmetric with respect to z–z axis. The temperature variation was increased from 0 to 60 °C with a 5 °C increment. The thermal load was applied on the whole surface of the cross section. The mechanical and physical properties of concrete such as the compressive strength f_{c28}, tensile strength f_{ct28}, Young's modulus E_c, the coefficient of thermal expansion α_c, concrete density γ_c, and Poisson's ratio ν_c are, respectively, equal to 40, 4.1 MPa, 28 GPa, 11.6×10^{-6}/°C, 2.4 g/cm^3, and 0.17. The Poisson's ratio in the longitudinal direction υ_{lt}, Poisson's ratio in the transverse direction υ_{tt}, transverse modulus of elasticity E_t, and transverse coefficient of thermal expansion α_{ft}, of GFRP bars are, respectively, equal to 0.28, 0.38, 7.1 GPa, and 33×10^{-6}/°C [3]. The modulus E_t and the coefficient ν_{tt} have been determined theoretically using the mixing rule. The other FRP mechanical properties such as ultimate tensile strength f_{fu}, the longitudinal modulus of elasticity E_l, and the ultimate tensile strain ε_{lu} are shown in Table 1. The mechanical properties of concrete and GFRP bars are those determined experimentally by Zaidi [3,5].

3 Analytical Model

Aiello [7], Zaidi [5,8], and Bellakehal [6] have developed analytical models based on Timoshenko's equations of linear elasticity theory for a hollow cylinder under internal hydrostatic pressure P, considering the in-plane stresses state [9]. This model has been adapted to this study to include the effect of the vertical overlap of FRP bars of prismatic beams on the stress distribution in the concrete cover and FRP bar under large temperature increase. In the case of concrete beams reinforced with two overlapped FRP bars (Fig. 2a), the circumferential tensile stresses due to the radial pressure in the first and the second bars, for a concrete element situated at a distance ρ from the center of each bar, are respectively given by the following equations:

$$\sigma_{t1}(\rho) = \frac{P_1}{r_1^2 - 1}\left(1 + \frac{b_1^2}{\rho^2}\right), \quad (1)$$

$$\sigma_{t2}(\rho) = \frac{P_2}{r_2^2 - 1}\left(1 + \frac{b_2^2}{\rho^2}\right), \quad (2)$$

where $r_1 = \frac{2c_1+d_b}{d_b}$; $r_2 = \frac{2c_2+d_b}{d_b}$; $b_1 = c_1 + a$; $b_2 = c_2 + a$; and $a = d_b/2$, c_1 and c_2 are respectively the concrete cover thicknesses of the first and second FRP bars. P_1 and P_2 refer to the radial pressure exerted by the first and the second FRP bars, respectively, which are given in Eqs. 3 and 4:

$$P_1 = \frac{(\alpha_t - \alpha_c)\Delta T}{\frac{1}{E_c}\left(\frac{r_1^2+1}{r_1^2-1} + \nu_c\right) + \frac{1}{E_t}(1 - \nu_{tt})}, \quad (3)$$

$$P_2 = \frac{(\alpha_t - \alpha_c)\Delta T}{\frac{1}{E_c}\left(\frac{r_2^2+1}{r_2^2-1} + \nu_c\right) + \frac{1}{E_t}(1 - \nu_{tt})}, \quad (4)$$

where $(\alpha_t - \alpha_c).\Delta T$ is the transverse differential thermal strain; α_t is the transverse coefficient of thermal expansion (TCTE) of FRP bar; and α_c is the TCTE of concrete.

The maximum circumferential tensile stress at the interface FRP bar/concrete (Zone 1) (Fig. 2b) due to the radial pressure of one bar (P_1), obtained from Eq. 1 for $\rho = a$, is given by the following equation:

$$\sigma_{t\max 1} = \frac{r_1^2 + 1}{r_1^2 - 1} P_1. \quad (5)$$

The circumferential tensile stress in concrete located in the interface line at the interaction zone (Zone 2), due to the radial pressure of the first bar P_1 and that of the second bar P_2, is estimated by:

$$\vec{\sigma}_t(\rho) = \vec{\sigma}_{t1}(\rho) + \vec{\sigma}_{t2}(\rho) \Rightarrow \sigma_t^2 = \sigma_{t1}^2 + \sigma_{t2}^2 + 2\sigma_{t1}\sigma_{t2}\cos(2\beta). \quad (6)$$

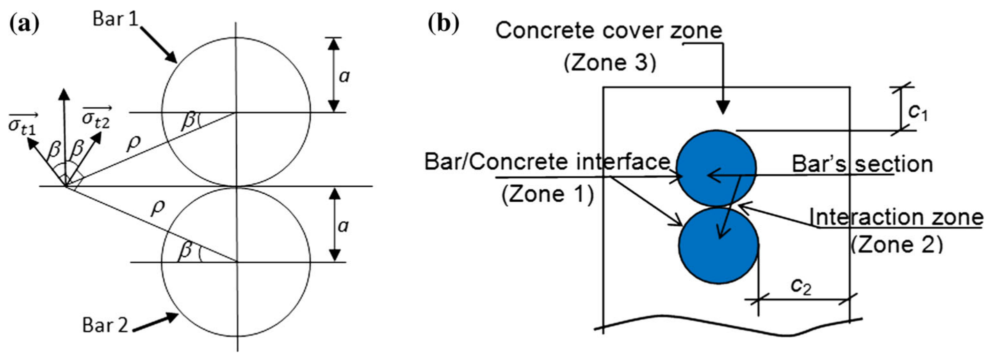

Fig. 2 Prismatic concrete beam reinforced with two GFRP bars: **a** presentation of stresses vectors. **b** Different areas considered in beam section

By substituting the expressions of σ_{t1} and σ_{t2} of Eqs. 1 and 2 in Eq. 6, the circumferential tensile stress of concrete located in FRP bars interaction zone is as follows:

$$\sigma_t^2(\rho) = \left[\frac{P_1}{r_1^2-1}\left(1+\frac{b_1^2}{\rho^2}\right)\right]^2 + \left[\frac{P_2}{r_2^2-1}\left(1+\frac{b_2^2}{\rho^2}\right)\right]^2 + \frac{2P_1P_2}{\left(r_1^2-1\right)\left(r_2^2-1\right)}\left(1+\frac{b_1^2}{\rho^2}\right)\left(1+\frac{b_2^2}{\rho^2}\right)\cos(2\beta). \quad (7)$$

The maximum circumferential tensile stress in FRP bar/concrete interface located in FRP bars interaction zone due to the pressure of the first bar P_1 and that of the second bar P_2, where ρ = a and $\beta = 0°$, is given by the following equation:

$$\sigma_{t\max 1,2}(a) = \sigma_{t1}(a) + \sigma_{t2}(a) = \frac{r_1^2+1}{r_1^2-1}P_1 + \frac{r_2^2+1}{r_2^2-1}P_2. \quad (8)$$

The first radial crack appears in the concrete at the interface FRP bar/concrete (Zone 1) when the circumferential stress reaches the tensile strength of concrete ($\sigma_{tmax1} = f_{ct}$). From Eqs. 3 and 5, we can write:

$$\Delta T_{cr1} = \frac{f_{ct}}{(\alpha_t - \alpha_c)}\left[\frac{1}{E_c} + \frac{r_1^2-1}{r_1^2+1}\left(\frac{\upsilon_c}{E_c} + \frac{1-\upsilon_{tt}}{E_t}\right)\right]. \quad (9)$$

In the case of concrete beams reinforced with two overlapped FRP bars, the temperature variation producing the first radial crack in the concrete at the interaction zone (Zone 2) is attained when $\sigma_{tmax1,2}$ reaches f_{ct}. Using Eqs. 3, 4, and 8, we get Eq. 10:

$$\Delta T_{cr2} = \frac{f_{ct}}{(\alpha_t - \alpha_c)}\left[\frac{\frac{r_1^2+1}{r_1^2-1}}{\frac{1}{E_c}\left(\frac{r_1^2+1}{r_1^2-1}+\nu_c\right)+\frac{1}{E_t}(1-\nu_{tt})} + \frac{\frac{r_2^2+1}{r_2^2-1}}{\frac{1}{E_c}\left(\frac{r_2^2+1}{r_2^2-1}+\nu_c\right)+\frac{1}{E_t}(1-\nu_{tt})}\right]^{-1}. \quad (10)$$

The circumferential strains ε_{ct} in concrete at the FRP bar/concrete interface (ρ = a) (Zone 1), due to the radial pressure P of one bar and the temperature variation ΔT, are given by:

$$\varepsilon_{ct} = \frac{P}{E_c}\left(\frac{r^2+1}{r^2-1}+\nu_c\right) + \alpha_c\Delta T. \quad (11)$$

The circumferential strains ε_{ct} in the concrete located in FRP bars interaction zone (Zone 2), due to the radial pressure of the first bar P_1 and that of the second bar P_2, and also to the temperature variation ΔT, are given by Eqs. 12 and 13.

$$\varepsilon_{ct} = \varepsilon_{ct1}(a) + \varepsilon_{ct2}(a) \quad (12)$$

$$\varepsilon_{ct} = \frac{P_1}{E_c}\left(\frac{r_1^2+1}{r_1^2-1}+\nu_c\right) + \frac{P_2}{E_c}\left(\frac{r_2^2+1}{r_2^2-1}+\nu_c\right) + \alpha_c\Delta T. \quad (13)$$

The circumferential strains ε_{ct} in the outer surface of the concrete cover (Zone 3) ($\rho = b_1$), due to the radial pressure P_1 and the temperature variation ΔT, are given by Eq. 14:

$$\varepsilon_{ct} = \frac{2P_1}{E_c(r_1^2-1)} + \alpha_c\Delta T. \quad (14)$$

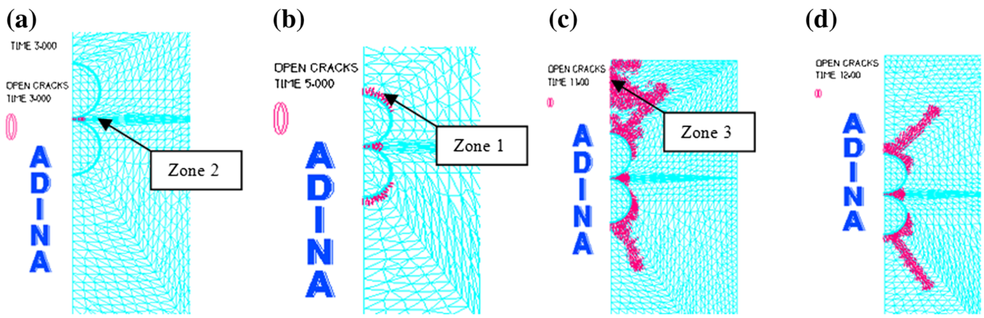

Fig. 3 Concrete cracking pattern of beams P.#13.20 (c/d_b=1.6) and P.#13.30(c/d_b=2.4): **a** appearance of the first radial cracks in Zone 2 at $\Delta T_{cr} = 15\,°C$. **b** Forming of the first radial cracks in Zone 1 at $\Delta T_{cr} = 25\,°C$. **c** A complete cracking of concrete cover at $\Delta T_{sp} = 55\,°C$ for beam P.#13.20, c/d_b=1.6. **d** Partial cracking of the concrete cover at $\Delta T = 60\,°C$ for beam P.#13.30, $c/d_b = 2.4$

Table 2 Cracking temperature variation ΔT_{cr} versus c/d_b ratio at FRP bar/concrete interface (Zone 1) and FRP bars interaction zone (Zone 2), and temperature variation ΔT_{sp} producing the total failure of concrete cover—comparison of analytical and numerical results

c/d_b	Analytical model		Numerical model		
	ΔT_{cr1} (°C)	ΔT_{cr2} (°C)	ΔT_{cr1} (°C)	ΔT_{cr2} (°C)	ΔT_{sp} (°C)
3.2	23.75	11.90	22.84	11.08	> 60
2.6	23.52	11.84	22.10	11.02	> 60
2.4	23.35	11.70	22.91	10.65	> 60
2.1	23.14	11.75	21.52	10.20	> 60
2.0	23.00	11.61	21.81	10.99	> 60
1.9	22.91	11.46	20.97	10.79	55
1.6	22.45	11.47	20.81	10.65	50
1.4	22.06	11.08	21.03	10.57	45
1.3	21.75	11.16	20.65	10.62	45
1.2	21.53	10.94	20.76	10.54	40
1.0	20.80	11.03	20.60	10.49	40

4 Analysis of Numerical Results

Figure 3a, b illustrates the temperature variation producing the first radial cracks in concrete (ΔT_{cr}) of beam P#13.20. Note that the first radial cracks appear at around $\Delta T_{cr} = 15°C$ in the bars interaction zone (Fig. 3a) and at around $\Delta T_{cr} = 25\,°C$ at FRP bar/concrete interface (Zone 1) (Fig. 3b).

Figure 3c, d illustrates the propagation of cracks in the concrete cover and the temperature variation producing the failure of concrete cover (ΔT_{sp}) of beams P.#13.20 and P.#13.30, respectively. Figure 3c shows that beam P.#13.20 had a complete cracking of concrete cover at a temperature variation of $\Delta T_{sp} = 55\,°C$. However, for beam P.#13.30, the complete rupture of the concrete cover was not observed up to $\Delta T = 60\,°C$; this is shown for all beams having ratio (c/d_b) greater than or equal to 2 (Fig. 3d and Table 2).

Figures 4 and 5 present typical curves showing the transverse thermal strains obtained from the numerical analysis of prismatic concrete beams reinforced with two overlapped GFRP bars, with c/d_b ratios varying from 1.0 to 3.2, and sub-

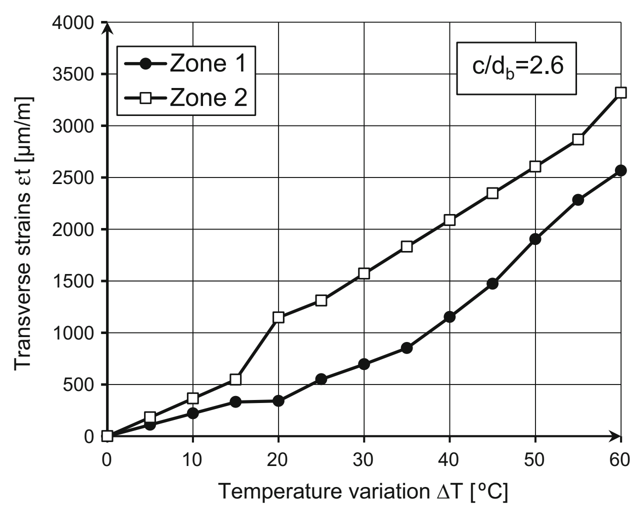

Fig. 4 Transverse strains of concrete versus a temperature variation at the FRP bar/concrete interface (Zone 1) and in FRP interaction zone (Zone 2) for a beam P.#10.25 having c/d_b=2.6

jected to large temperature increase. These typical curves present a comparison between strains obtained at the FRP

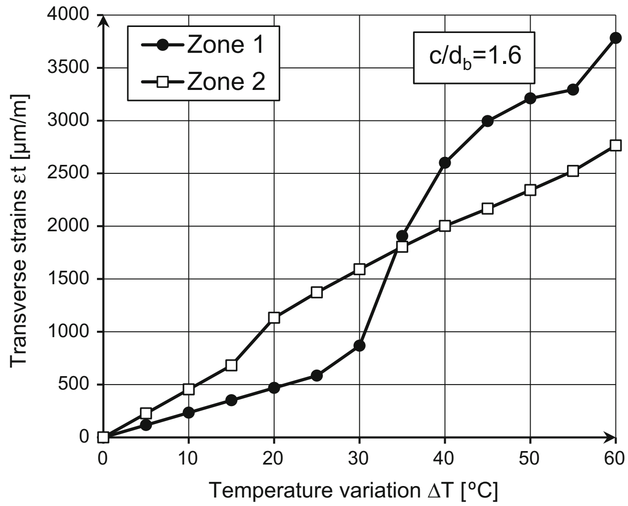

Fig. 5 Transverse strains of concrete versus a temperature variation at the FRP bar/concrete interface (Zone 1) and in FRP interaction zone (Zone 2) for a beam P.#16.25 having c/d_{b}=1.6

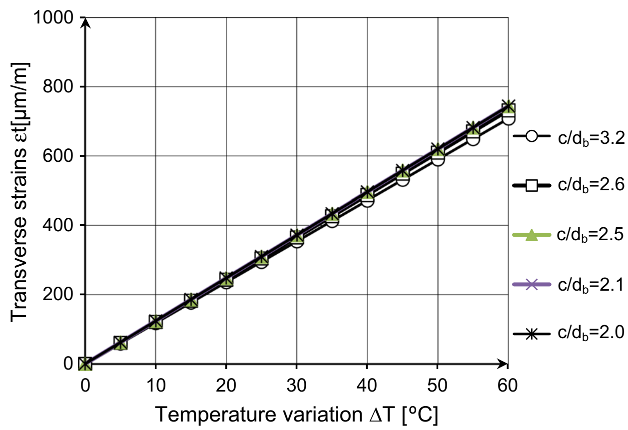

Fig. 6 Transverse strains of concrete versus a temperature variation at the outer surface of concrete cover for $2 \leq c/d_{\mathrm{b}} \leq 3.2$

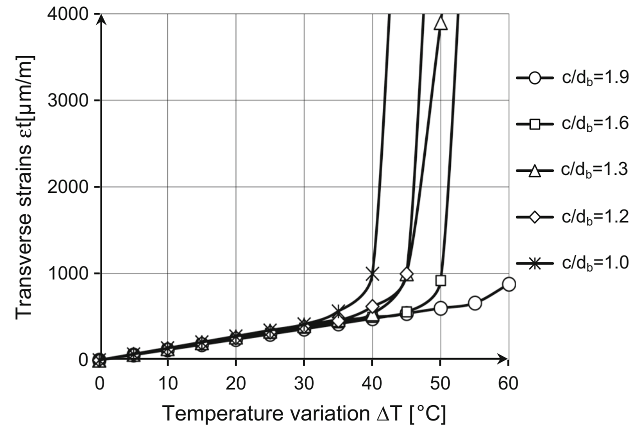

Fig. 7 Transverse strains of concrete versus a temperature variation at the outer surface of concrete cover for $1 \leq c/d_{\mathrm{b}} \leq 1.9$

bar/concrete interface (Zone 1) and those obtained in bars interaction zone (Zone 2). It is observed that the transverse thermal strains in Zones 1 and 2 are linear up to a temperature variation of around 25 and 15 °C, respectively. These temperatures represent the temperature variations producing the first crack at the appropriate interface (Fig. 3a, b) from which the strain curves become nonlinear due to the formation of cracks in the concrete surrounding the GFRP bars.

It can be seen that the transverse thermal strains in the interaction zone (Zone 2) are generally greater than those in Zone 1, particularly before the failure of concrete cover because this area is subject to a high concentration of tensile stresses due to the dual action of radial pressure exerted by both GFRP bars under large temperature increase. Additionally, it can be noted that the transverse thermal strains in Zone 1 increase suddenly at ΔT around 30 and 40 °C depending on the ratio c/d_{b}. This is due to the development of deep cracks within the concrete surrounding the GFRP bars, particularly for ratios c/d_{b} less than 2 (Fig. 3c, d).

According to Figs. 6 and 7, it is noted that the transverse thermal strains at the outer surface of concrete cover (Zone 3) are linear for beams having a ratio $c/d_{\mathrm{b}} \geq 2$, because no cracks reached the outer surface of concrete cover for these beams (Fig. 3d and Table 2). However, for ratios $c/d_b < 2$, it can be seen that the transverse thermal strains are linear up to a temperature variation of about ΔT_{sp}(temperature variation producing the total failure of concrete cover) beyond which the strain curves become nonlinear due to the formation of cracks reaching the outer surface of concrete cover. Thus, it can be concluded that ratios c/d_{b} greater than 1.9 are sufficient to avoid the failure of concrete cover of prismatic concrete beams reinforced with two FRP bars vertically overlapped. Figure 7 shows also that the temperature variation ΔT_{sp} produces the total failure of concrete cover decreases significantly with the decrease in c/d_{b} ratio (Table 2).

5 Comparison of Analytical and Numerical Results

5.1 Temperature Variation Producing the First Crack

Table 2 presents a comparison between analytical and numerical results in terms of temperature variations ΔT_{cr1} and ΔT_{cr2} producing the first radial crack at the FRP bar/concrete interface (Zone 1) and at the FRP bars interaction zone (Zone 2), respectively, by varying the ratio c/d_{b} from 1.0 to 3.2. From this table, it can be observed that the ΔT_{cr} increases slightly with the increase in the ratio c/d_{b}. Moreover, the values obtained from the analytical model are very close to those predicted in the numerical model. Consequently, it can be concluded that the approach used to develop Eq. 6 is appropriate. It means that the stress in the interaction zone is the

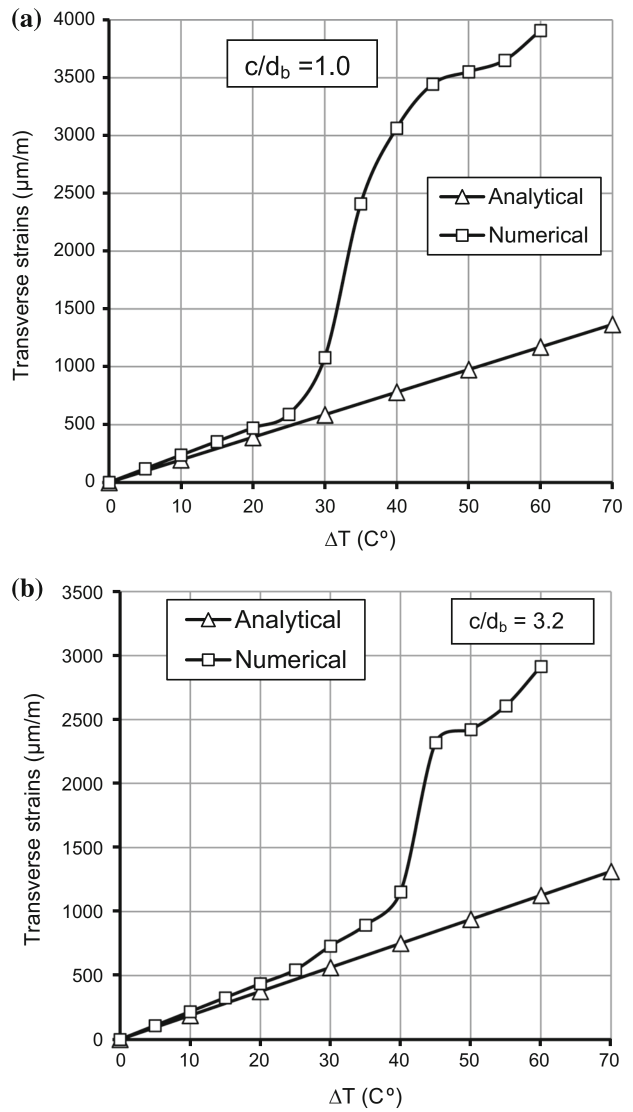

Fig. 8 Transverse thermal strains of concrete at the FRP bar/concrete interface (Zone 1)—comparison of analytical and numerical results for beam **a** P.#19.20 having $c/d_\mathrm{b} = 1$, **b** P.#10.30 having $c/d_\mathrm{b} = 3.2$

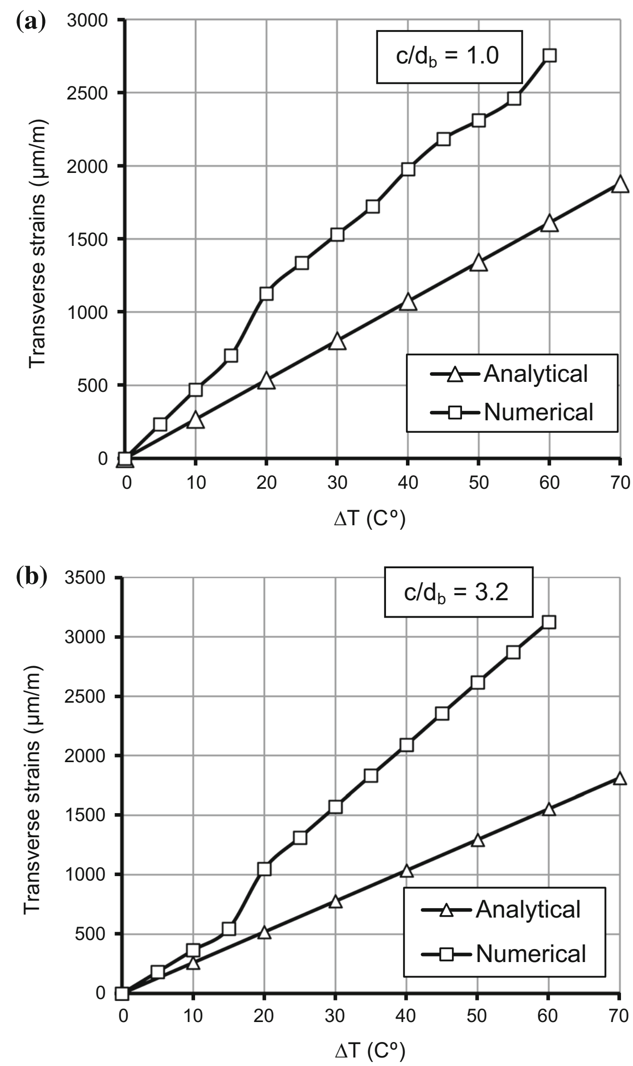

Fig. 9 Transverse thermal strains of concrete in FRP bars interaction zone (Zone 2)—comparison of analytical and numerical results for beam **a** P.#19.20 having $c/d_\mathrm{b} = 1$, **b** P.#10.30 having c/d_b=3.2

superposition of both FRP bar stresses. As shown in Table 2, ΔT_{cr1} values are greater than those of ΔT_{cr2}. This is due to the concentration of thermal stresses in the interaction zone. So, the first cracks appear at a temperature of 42°C ± 2°C (since the reference temperature is 20°C) for concrete beams reinforced with no overlapped FRP bars. However, if these beams are reinforced by overlapped bars, this temperature is 31°C ± 1°C. Therefore, the overlap of FRP bars reduces the temperature producing the first crack. It should be noted that the first crack occurs in the concrete at FRP bar/concrete interface in both zones when the circumferential tensile stress of concrete reaches the tensile strength of concrete (f_{ct}) which is considered equal to 4.1 MPa [12].

5.2 Transverse Thermal Strains

Figures 8, 9, and 10 are typical curves that present a comparison between analytical and numerical results in terms of transversal thermal strains of concrete, respectively, at FRP bar/concrete interface (Zone 1), in FRP bars interaction zone (Zone 2), and at the outer surface of concrete cover (Zone 3) of concrete beams reinforced with two vertically overlapped GFRP bars, and having a ratio of concrete cover thickness to FRP bar diameter c/d_b ranging from 1.0 to 3.2. From these figures, it can be seen that the transverse strain curves obtained from the nonlinear numerical model are almost similar to those obtained from the linear analytical model for temperature variation less than ΔT_cr which is equal to 25, 15, and 40 °C for Zones 1, 2, and 3, respectively. Beyond these temperatures, the strain values predicted by the numerical

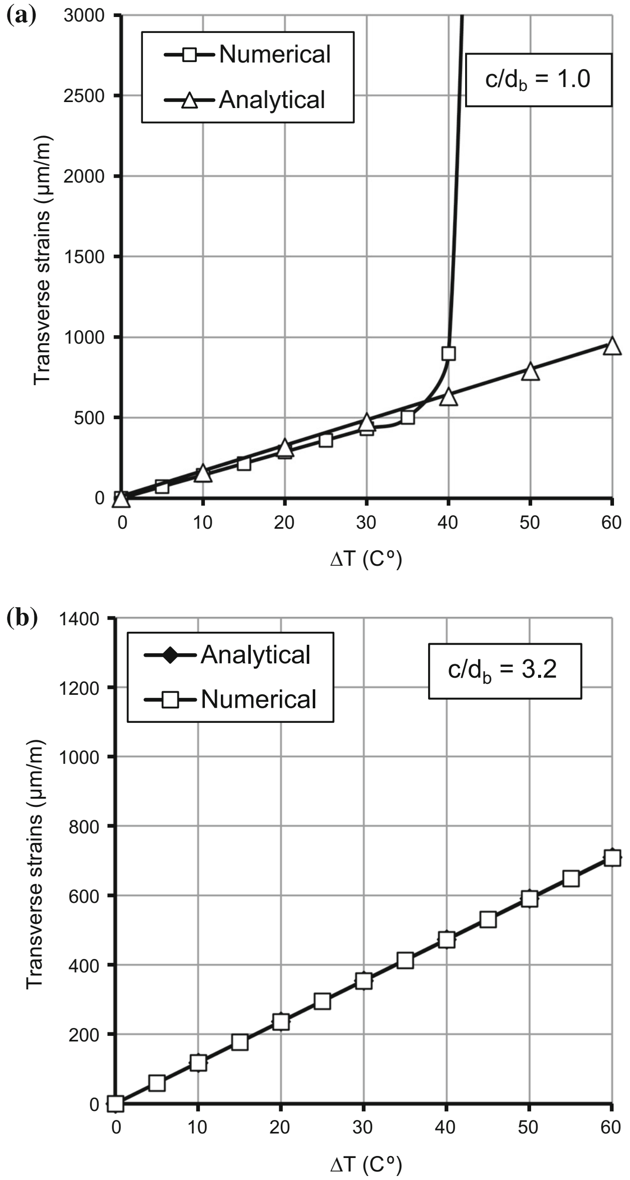

Fig. 10 Transverse thermal strains of concrete at the outer surface of concrete cover (Zone 3)—comparison of analytical and numerical results for beam **a** P.#19.20 having c/d_b=1, **b** P.#10.30 having c/d_b=3.2

model are by far higher than those predicted by the analytical model due to the presence of cracks in concrete which have not been considered by the analytical model.

6 Conclusions

The results obtained from this analytical and numerical study analyzing the vertical overlap effect of two GFRP bars embedded in prismatic concrete beams having c/d_b ratio ranging from 1.0 to 3.2 and concrete tensile strength of 4.1 MPa, under a temperature variation up to 60 °C, allowed drawing the following conclusions:

1. According to analytical and numerical results, the first cracks appear within concrete at FRP bar/concrete interface at a temperature of 42 °C(Δ T $=$ 22 °C since the reference temperature T_o $=$ 20 °C) for concrete beams reinforced with no overlapped FRP bar. However, the cracking temperature is 31 °C (ΔT $=$ 11 °C) if these beams are reinforced by overlapped FRP bars. This is due to the high concentration of tensile stresses in concrete zone between FRP bars generated by the dual pressure exerted by both GFRP bars under large temperature increase.
2. For transverse thermal strains at FRP bar/concrete interface (Zone 1) and FRP bars interaction zone (Zone 2), the numerical results are in line with the analytical results for thermal loads less than cracking thermal loads. Beyond cracking thermal loads, the numerical results are higher due to the appearance of radial cracks in concrete.
3. According to the nonlinear numerical model, the thermal loads ΔT_{sp} producing the failure of concrete cover are 40, 45, and 55 °C, corresponding to the ratio of concrete cover thickness to FRP bar diameter (c/d_b) of 1, 1.4, and 1.9, respectively. A c/d_b ratio which is higher than 1.9 is sufficient to avoid failure of the concrete cover of prismatic concrete beams reinforced with two vertically overlapped GFRP bars under thermal loads up to 60 °C.
4. For transverse thermal strains in the outer surface of the concrete cover (Zone 3), the numerical results are in good agreement with the analytical results up to the temperature variation producing the total failure of concrete cover (ΔT_{sp} $\geq$ 40 °C), from which numerical results are relatively large due to the presence of cracks reaching the outer surface of concrete cover that were not considered in the linear analytical model.
5. The temperature variation ΔT_{cr} producing the first cracks slightly decreases with the decrease in c/d_b ratio. But the temperature variation ΔT_{sp} produces a total failure of concrete cover decreases significantly with the decrease in c/d_b ratio.

References

1. EL-Zaroug, O.; Forth, J.; Ye, J.: Flexural performance of concrete slabs reinforced with GFRP and subjected to different thermal histories. Paper presented at 8th international symposium on FRP for reinforcement of concrete structures (FRPRCS-8), University of Patras, Patras, Greece (2007)
2. Canadian Standards Association (CSA). Design and construction of building structures with fibre-reinforced polymers, CAN/CSA–S806–12, Mississauga, Ontario, Canada (2012)

3. Masmoudi, R.; Zaidi, A.; Gérard, P.: Transverse thermal expansion of FRP bars embedded in concrete. J. Compos. Constr. **9**(5), 377–387 (2005)
4. Galati, N.; Nanni, A.; Focacci, F.: Thermal effects on bond between FRP rebars and concrete. Compos. Part A **37**(8), 1223–1230 (2006)
5. Zaidi, A.; Masmoudi, R.: Thermal effect on fiber reinforced polymer reinforced concrete slabs. Can. J. Civ. Eng. **35**, 312–320 (2008)
6. Bellakehal, H.; Zaidi, A.; Masmoudi, R.; Bouhicha, M.: Behavior of FRP bars-reinforced concrete slabs under temperature and sustained load effects. Polym. J. **6**, 873–889 (2014)
7. Aiello, M.A.; Focacci, F.; Nanni, A.: Effects of thermal loads on concrete cover of fiber reinforced polymer reinforced elements: theoretical and experimental analysis. ACI Mater. J. **98**(4), 332–339 (2001)
8. Zaidi, A.; Mouattah, K.; Masmoudi, R.: Finite element modeling of fiber reinforced polymer bars embedded in prismatic concrete beams under high temperatures. J. Reinf. Plast. Compos. **34**(4), 315–328 (2015)
9. Timoshenko, S.P.; Goodier, J.N.: Theory of Elasticity. Mc-Graw-Hill Book Company, New York (1970)
10. Zaidi, A.; Masmoudi, R.; Bouhaicha, M.: Finite element analysis of thermal deformations in concrete surrounding FRP bars under low temperature. Paper presented at 8th international conference on short and medium span bridges, Niagara Falls, Canada (2010)
11. Zaidi, A.; Masmoudi, R.: Numerical analysis of thermal behavior of concrete cover around FRP-bars in cold region. Arab. J. Sci. Eng. **37**(2), 489–504 (2012)
12. Bellakehal, H; Zaidi, A.; Masmoudi, R.; Mouattah, K.; Boutaiba, A.; Bencheriet, M.: Analyse Numérique des Contraintes Thermiques des Barres en PRF Chevauchées et Ancrées dans le Béton. Paper presented at 13th Arab structural engineering conference, University of Blida, Algeria (2015)